

UC Irvine

UC Irvine Previously Published Works

Title

Chapter 7 Visualizing retinoic acid morphogen gradients

Permalink

<https://escholarship.org/uc/item/1h6505m7>

Authors

Schilling, TF

Sosnik, J

Nie, Q

Publication Date

2016

DOI

10.1016/bs.mcb.2016.03.003

Peer reviewed



Published in final edited form as:

Methods Cell Biol. 2016 ; 133: 139–163. doi:10.1016/bs.mcb.2016.03.003.

Visualizing retinoic acid morphogen gradients

T.F. Schilling¹, J. Sosnik, and Q. Nie

University of California, Irvine, CA, United States

Abstract

Morphogens were originally defined as secreted signaling molecules that diffuse from local sources to form concentration gradients, which specify multiple cell fates. More recently morphogen gradients have been shown to incorporate a range of mechanisms including short-range signal activation, transcriptional/translational feedback, and temporal windows of target gene induction. Many critical cell–cell signals implicated in both embryonic development and disease, such as Wnt, fibroblast growth factor (Fgf), hedgehog (Hh), transforming growth factor beta (TGF β), and retinoic acid (RA), are thought to act as morphogens, but key information on signal propagation and ligand distribution has been lacking for most. The zebrafish provides unique advantages for genetics and imaging to address gradients during early embryonic stages when morphogens help establish major body axes. This has been particularly informative for RA, where RA response elements (RAREs) driving fluorescent reporters as well as Fluorescence Resonance Energy Transfer (FRET) reporters of receptor binding have provided evidence for gradients, as well as regulatory mechanisms that attenuate noise and enhance gradient robustness *in vivo*. Here we summarize available tools in zebrafish and discuss their utility for studying dynamic regulation of RA morphogen gradients, through combined experimental and computational approaches.

INTRODUCTION

Signals that determine multiple cell fates in a concentration-dependent manner are known as morphogens. Many of the major cell-signaling pathways studied in biology—Wnt, Fgf, Tgfb, etc.—work this way in some contexts. The morphogen gradient is a fundamental concept in developmental biology, originally described by Lewis Wolpert’s “French Flag” model for the developing chick limb bud, in which cells interpret different threshold concentrations of morphogen resulting in distinct fates (Fig. 1A) (Tickle, Summerbell, & Wolpert, 1975). However, the mechanisms producing morphogen gradients are probably diverse. What evidence is required to validate Wolpert’s model for a given morphogen? To start with, it needs to be present as a gradient, and the perceived gradient needs to translate into gene expression activation thresholds. Furthermore for Wolpert’s model to work as intended recent studies have revealed additional constraints: shaping the gradient, making its response robust, creating sharp gene expression boundaries, and dealing with biological noise (Lander, 2007; Meinhardt, 2009; Wartlick, Kicheva, & Gonzalez-Galtan, 2009). Can fields of cells really generate smooth gradients such as Wolpert envisioned or are they noisy

¹Corresponding author: tschilli@uci.edu.

(Fig. 1B)? If the answer is the latter, as seems likely, how do sharp boundaries of gene expression form in the face of variability in signal production, cellular architecture, and environmental fluctuations?

1. CHALLENGES FOR MORPHOGEN GRADIENT STUDIES

The problem is more complex than it appears at face value. Recent studies have revealed unexpected dynamics of both ligand and response, positive and negative feedback, and mechanisms for scaling gradients to adjust for changes in tissue size and shape (Fig. 1C,D) (Ben-Zvi, Shilo, & Barkai, 2011; Briscoe & Small, 2015; Horinaka & Morishita, 2012; Meinhardt, 2015). Gene regulatory networks that specify different cell fates based on concentration may elicit different responses depending on regulatory mechanisms (eg, feedback) within the network (Horinaka & Morishita, 2012). For example, positive feedback loops can generate bistability, where cells transition through a less stable state as the morphogen signal increases (Fig. 1C). This may help sharpen boundaries of target gene expression through switchlike responses. In contrast, negative feedback can cause oscillations due to cyclical levels of inhibition, which leads to periodic patterns (Fig. 1C). Two or more signals may also act in parallel, such as a combination of activation and inhibition, leading to responses only within a middle range of input (Horinaka & Morishita, 2012).

These regulatory mechanisms remain largely unknown for most putative morphogens. In fact it remains controversial if they even form gradients, and few studies have examined their spatial and temporal dynamics (Stathopoulos & Iber, 2013). The best studied is Bicoid in *Drosophila*, which clearly forms a gradient of nuclear protein along the anterior–posterior (A–P) axis in the early embryo (Driever & Nusslein-Volhard, 1988a, 1988b; Grimm, Coppey, & Wieschaus, 2010). But this is an unusual case in that Bicoid is a transcription factor, which forms a cytoplasmic gradient within a syncytium. For the more common secreted, extracellular morphogens (eg, Bmps, Fgfs, Wnts, Shh), research has relied on indirect methods to visualize the ligands or their cellular responses (eg, fluorescently tagged ligands and reporters), due to technical limitations in imaging the molecules involved directly (Alexander et al., 2011; Balasubramanian & Zhang, 2015; Bokel & Brand, 2013; Briscoe & Small, 2015; Muller et al., 2012; Ramel & Hill, 2013; Strigini & Cohen, 2000; Tuazon & Mullins, 2015). Most of these visualization methods cannot detect changes on rapid timescales. They also may miss fine cellular processes that provide direct contacts between signaling and responding cells (Prols, Sagar, & Scaal, 2015). Recent studies call into question several classic peptide morphogens, including Wg in the *Drosophila* wing disc where a membrane-tethered form can suffice for function (Alexandre, Baena-Lopez, & Vincent, 2014), and Shh in the vertebrate neural tube, where cell rearrangements rather than concentration thresholds can account for many fate outcomes (Xiong et al., 2013). There is also growing recognition that signals are noisy from embryo to embryo and from cell to cell. How do cells interpret signals in the face of stochastic fluctuations in both space and time?

One putative nonpolypeptide morphogen that has stood the test of time is the vitamin A derivative, retinoic acid (RA). RA influences the behaviors of many cell types in embryos (eg, heart, gut, somites, hindbrain, craniofacial skeleton), as well as adult stem cells (eg,

neural, pancreatic), cancers (leukemia), and regenerating organs (cardiomyocytes) (Rhinn & Dolle, 2012; White & Schilling, 2008). One of the best-studied roles for RA is in anterior–posterior (A–P) patterning during vertebrate gastrulation, where it acts in parallel with Fgfs and Wnts to promote posterior development, particularly in the developing hindbrain (Kudoh, Wilson, & Dawid, 2002; Schilling, Nie, & Lander, 2012). In this context, RA fits all of the major morphogen criteria, acting at long range to determine multiple cell fates in a concentration-dependent manner. Here we summarize recent work in zebrafish combining developmental genetics, new imaging methods, and computational modeling of hindbrain development to reveal an integrated signaling network that can help explain RA’s dynamics and precision as a morphogen.

2. FEEDBACK ALLOWS RETINOIC ACID TO ACT AS A GRADED MORPHOGEN

The shapes of morphogen gradients are determined by the source of the ligand, its rate of production, transport properties, and stability (Ben-Zvi & Barkai, 2010; Sample & Shvartsman, 2010; Umulis, Shimmi, O’Connor, & Othmer, 2010). Gradient shape also depends on feedback mechanisms such as self-enhanced receptor-mediated degradation, which helps make gradients robust—ie, able to compensate for variability in morphogen availability. This has been demonstrated for growth factors of the TGF β , Wg, and Hh families (Eldar, Rosin, Shilo, & Barkai, 2003; Meinhardt, 2009; Wartlick et al., 2009).

Both positive and negative feedback are critical for RA signaling (Fig. 2A) (Rhinn & Dolle, 2012; White & Schilling, 2008). Unlike polypeptide morphogens, RA is a lipophilic vitamin A derivative synthesized by aldehyde dehydrogenases (Aldhs) and degraded by cytochrome p450s (Cyp26s) within cells. Once synthesized, extracellular and intracellular binding proteins (RBPs, CRABPs) bind to, solubilize, and transport RA first into the cytoplasm and then into the nucleus where it binds nuclear hormone receptors (RARs, RXRs). RA negatively regulates its own synthesis by Aldh1a2 and positively regulates both its precursors (eg, Lrat) and receptors (RARs) (Fig. 2A). How does this influence A–P patterning of the developing hindbrain?

Morphogen gradients typically include local sources of ligand production and tightly regulated ligand degradation (Briscoe & Small, 2015; Lander, 2007; Meinhardt, 2015). For RA and A–P patterning of the hindbrain, this arrangement occurs during gastrulation. In all vertebrates, RA is synthesized posteriorly in the mesoderm (*aldh1a2* expression) and degraded anteriorly in the future forebrain/midbrain (*cyp26a1* expression), as exemplified in a zebrafish embryo at 8 h postfertilization (hpf) (Schilling et al., 2012; White, Nie, Lander, & Schilling, 2007). This suggests that RA travels from source to sink across the future hindbrain territory to establish a gradient. Most studies have focused on the potential steady-state gradients that this arrangement would produce, but as we discuss below temporal (pre-steady state) dynamics may be just as, if not more, important for hindbrain segmentation.

Evidence for an RA morphogen gradient in hindbrain development is strong. The hindbrain consists of eight segments (rhombomeres), each containing different types of interneurons and motor neurons that prefigure the cranial nerves (Fig. 2B) (Lumsden and Keynes, 1989;

Trevarrow, Marks, & Kimmel, 1990). Aldh1a2 expression is restricted to the mesoderm flanking the posterior hindbrain/anterior spinal cord where it converts vitamin A into RA. This RA then diffuses or is transported anteriorly where it directly regulates transcription factors that specify different rhombomeres. Dietary depletion of vitamin A in chick embryos or loss-of-function mutations in Aldh1a2, both in zebrafish and mice, lead to a loss of posterior and expansion of anterior rhombomeres (Begemann, Schilling, Rauch, Geisler, & Ingham, 2001; Niederreither, Vermot, Schuhbauer, Chambon, & Dolle, 2000; White & Schilling, 2008). Conversely treating embryos with exogenous RA expands posterior at the expense of anterior rhombomeres. Importantly both loss- and gain-of-function approaches are dose dependent—higher doses of pharmacological inhibitors of Aldhs or RA treatments lead to progressively more severe anteriorization or posteriorization, respectively.

3. CYP26S AS KEY REGULATORS OF RETINOIC ACID GRADIENT FORMATION

How does RA degradation influence its gradient properties? Morphogen models typically require some form of tightly controlled ligand removal (Lander, 2007; Briscoe & Small, 2015). Patterns of Cyp26a1 expression suggest that it forms an anterior sink for RA at the anterior end of the hindbrain. Analyses of transgenic reporters of RA signal activation in mice (RARE-lacZ) during hindbrain segmentation have suggested that “shifting boundaries” of two other RA-degrading enzymes, Cyp26b1 and Cyp26c1, progressively establish more posterior rhombomeres (Fig. 2C) (Sirbu, Gresh, Barra, & Duester, 2005). Functional studies of these three enzymes in zebrafish have shown that while loss of any one Cyp26 causes mild hindbrain defects, a loss of all three transforms the entire hindbrain into an r6/7 fate (Hernandez, Putzke, Myers, Margaretha, & Moens, 2007). While these two studies confirm the importance of RA degradation in patterning, the authors also argue for a model in which domains of RA degradation, rather than a gradient per se, pattern rhombomeres. Hernandez et al (Hernandez et al., 2007) point out that a gradient model seems inconsistent with the fact that in embryos devoid of RA (ie, DEAB treated to inhibit RA synthesis), exposure to a uniform concentration of exogenous RA can restore normal patterning. This calls the morphogen model for RA in the hindbrain into question.

However, these studies (Hernandez et al., 2007; Sirbu et al., 2005) fail to take into account one critical feature of any such morphogen system, feedback. In this case the focus of feedback is at the level of degradation. Hints at this come from the observation that RA induces Cyp26a1 expression, and that the range over which RA induces target gene expression increases upon Cyp26a1 inhibition (White et al., 2007). Cyp26a1 is also expressed at lower levels throughout the hindbrain field, and inhibited by two other posteriorizing signals, Fgf and Wnt (Kudoh et al., 2002). This forms the basis for a new, modified version of the gradient model in which self-enhanced degradation of RA forms part of an integrated network of posteriorizing signals (Fig. 2D) (White et al., 2007). Computational models confirm that this integrated system can account for many of the observed results, such as the restoration of a gradient in the presence of uniform, exogenous RA. Such a system is also robust to fluctuations in RA levels and “scales,” eg, it adapts as the hindbrain grows and the proximity of source and sink change (see Fig. 1D).

4. VISUALIZING THE RETINOIC ACID GRADIENT

These results beg the question of the nature of the gradient itself. Does it occur at the level of extracellular or intracellular RA? What is its shape? Unlike most putative morphogens, which are peptidic and synthesized de novo in developing embryos, RA presents additional challenges when it comes to microscopic observation. RA is a small lipophilic molecule that results from two consecutive enzymatic reactions that modify vitamin A of dietary origin (see Fig. 2A). Thus unlike Wnts or Fgfs, genetically encoded versions of fluorescently tagged RA cannot be generated. These characteristics have driven alternative strategies for visualizing RA signaling, most notably RA-response elements (RAREs) found in direct transcriptional targets of RA receptors driving lacZ or fluorescent reporters (Fig. 3). In mice a triplet of concatenated RAREs derived from the RAR β receptor, along with a minimal heat shock promoter, driving lacZ has been used for decades to detect RA in the nM range (Rossant, Zirngibl, Cado, Shago, & Giguere, 1991; Sirbu et al., 2005). In zebrafish, a similar transgenic construct driving eYFP (3xRARE:eYFP) responds to RA in the same range (Fig. 3B) (Perz-Edwards, Hardison, & Linney, 2001). Analysis of 3xRARE:eYFP reveals a graded response at the hindbrain/spinal cord junction that falls off rapidly at the level of r7 (Fig. 3C) (White et al., 2007). However, it fails to detect an RA gradient further anteriorly, across the developing hindbrain field, or elsewhere that RA is known to act. This is likely due to a lack of sufficient sensitivity of the 3xRARE:eYFP reporter. More recent attempts to generate better RA reporters in zebrafish have created transgenes with more concatenated copies of RARE, promoters of other RA target genes such as Cyp26a1, or the ligand-binding domain of RAR driving another transcriptional activator and its target sequences, to try and amplify the signal (Table 1) (Huang et al., 2014; Li et al., 2012; Mandal et al., 2013; Waxman & Yelon, 2011). However, while some of these transgenics report more broadly, none show clear gradients.

Recently the Miyawaki laboratory at the RIKEN institute in Saitama, Japan, has developed Genetically Encoded reporter Probes for RA (GEPRA) (Fig. 3D) (Shimozono, Iimura, Kitaguchi, Higashijima, & Miyawaki, 2013). These fusion proteins are composed of the RA binding pocket of an RAR with blue and yellow fluorescent proteins in their C- and N-termini. These reporters function based on Fluorescence Resonance Energy Transfer (FRET) between the fluorescent proteins (CFP, YFP) that surround the binding pocket. RA binding changes the reporter conformation, which alters the resonance energy transfer. This is directly proportional to RA levels, and therefore allows visualization of the distribution of RA in vivo, revealing gradients in developing zebrafish embryos (Fig. 3E and F). Consistent with previous studies, these gradients appear during gastrulation and are eliminated by inhibiting RA synthesis. Furthermore the highest RA levels occur near the head-trunk boundary and decline both anteriorly, across the future hindbrain field, and posteriorly across the developing somitic mesoderm, after gastrulation. Interestingly depleting GEPRA-B transgenics of RA (with DEAB) and simultaneously bathing them in uniform RA reestablishes a clear RA gradient by 10–11 hpf (three to four somites) (Fig. 3G) (Shimozono et al., 2013). These results provide strong evidence for the morphogen gradient model for RA.

However, while these GEPRA reporters have proven to be powerful tools to study RA, they have limitations. Because they rely on RA binding to the reporter, the measurements obtained are indirect—the actual microscopic observations depend on the fluorescence of the reporter and sensitivity of detection—ie, they depend on ratiometric imaging of CFP/YFP. This means that the results obtained depend on the reporter's dissociation constant (K_d ; Fig. 3E). Because different reporters have different K_d , Shimozone et al. (2013) report different RA gradient shapes depending on which reporter construct is used. In addition, because they depend on K_d , the association/dissociation times of GEPRA overlap with the temporal fluctuations of RA and render these reporters unsuitable for accurate temporal analyses. Future studies, such as Fluorescence Lifetime Microscopy to visualize RA autofluorescence, have the potential to analyze such gradient dynamics (Stringari et al., 2011).

5. CRABPS AND RETINOIC ACID SIGNAL ROBUSTNESS

Previous studies of morphogens have largely treated cells as perfect detectors of invariant signals, but this is almost certainly never the case (Briscoe & Small, 2015; Horinaka & Morishita, 2012; Lander, 2007; Meinhardt, 2009; Wartlick et al., 2009). The concept of “robustness” in this context in embryonic development refers to the relative insensitivity of pattern formation to variability and uncertainty, such as from environmental factors (temperature, nutrition), genetic differences, or the stochastic nature of biochemical processes. One might expect this to be particularly problematic for a signal like RA, which derives from vitamin A in the diet (White & Schilling, 2008). This issue also relates to the problem of scaling. How does the RA morphogen gradient adapt to changes in the size and shape of the hindbrain?

General strategies for studying robustness and scaling involve finding mechanisms that control ligand distribution or modulate cellular responses to the signal. How are the source and rate of ligand production controlled, how is it transported, and what determines its stability (Ben-Zvi & Barkai, 2010; Sample & Shvartsman, 2010; Umulis et al., 2010)? A common feedback mechanism involving self-enhanced receptor-mediated degradation has been shown to improve robustness for many growth factors including TGF β , Wg, and Hh (Eldar et al., 2003; Meinhardt, 2009; Wartlick et al., 2009).

Prime candidates for an analogous robustness mechanism in the RA system are the Cyp26s, which degrade intracellular RA. Our experimental results suggest that the RA gradient critically depends on self-enhanced degradation for gradient maintenance (Fig. 2D) (White et al., 2007) and this depends on Cyp26a1, which is induced by RA (Fig. 4A) and limits the range of RA action (Fig. 4B). Our computational models, in which we include known parameters for RA diffusion, transport and signal transduction, show that self-enhanced degradation makes the gradient at least twofold more robust to changes in RA synthesis than the case without degradation (although this results in a much smaller change in RA gradient slope).

The other prime candidates are the RA binding proteins, which solubilize RA and transport it both extracellularly (RBPs) and intracellularly (Crabps) (see Fig. 2A) (Astrom et al., 1991; Budhu, Gillilan, & Noy, 2001; Budhu & Noy, 2002; Delva et al., 1999). Studies in mice

have failed to find any functional requirements for the two Crabps, Crabp1 and Crabp2 (Lampron et al., 1995). In contrast, studies in zebrafish have shown that Crabp2a is RA inducible and required for robustness (Fig. 4C and D) (Cai et al., 2012). Similar to Cyp26a1, Crabp2a can negatively regulate RA signaling, since depleting it from zebrafish embryos makes them hypersensitive to small amounts of exogenous RA. 1 nM RA, which normally has no effect on wild-type embryos, induces RARE-YFP throughout the CNS in Crabp2a-deficient embryos. Thus like Cyp26a1, negative feedback through induction of Crabp2a dramatically improves the robustness of the response to RA.

Computational models predict that only the presence of a Crabp that acts negatively in the pathway can improve signal robustness to this extent, perhaps buffering RA in the cytoplasm away from its nuclear receptors (Fig. 4E) (Cai et al., 2012). We have used models based on known kinetics of RA interactions with RARs, Crabps, and Cyp26s to explore the effects of differing levels of RA synthesis on the resulting gradients (Fig. 4F). We calculate a robustness index (E) based on the difference in slope between the gradients generated by different levels of RA synthesis—which cross the same thresholds at different locations along the A–P axis. We derive E by calculating the normalized mean horizontal shift between the two gradients—where they cross 20% and 80% thresholds—and more robust gradients will have lower E values. This approach has the advantage that it integrates spatial information across the entire gradient as opposed to a single threshold. Crabp2a could buffer RA in the cytoplasm, preventing its nuclear localization, or it could promote RA degradation. Our models predict that Crabp2a promotes RA degradation, ie, by varying the corresponding parameters the most severe effects occur when varying the ability of Crabp2a to deliver RA to Cyp26s (Fig. 4F). Thus, the combined activities of Crabp2a and Cyp26a1 significantly improve the robustness of RA patterning in response to large variations in RA synthesis.

6. SHARPENING BOUNDARIES OF GENE EXPRESSION IN RESPONSE TO RETINOIC ACID GRADIENTS

Morphogens ultimately function to specify distinct spatial domains of gene expression and do it accurately from embryo to embryo. However, this robustness comes at a cost. Any morphogen gradient becomes shallower in slope further away from its source and more susceptible to stochastic fluctuations (ie, noise). Cells near future gene expression boundaries experience noise in morphogen concentration, ability to respond (eg, number of receptors), transcription/translation of target genes, and feedback (Elowitz, Levine, Siggia, & Swain, 2002; Kaern, Elston, Blake, & Collins, 2005; Kepler & Elston, 2001). In spatial patterning systems, noise is generally considered as detrimental.

Yet even boundaries far from the morphogen source eventually become razor sharp, leading to the question of exactly how these domains of gene expression sharpen? Our computational models predict that boundary sharpening the zebrafish hindbrain occurs via transition zones, in which cells express a mixture of genes eventually restricted to the anterior or posterior sides of the boundary (Fig. 5A) (Zhang et al., 2012). Sharpening requires large changes in gene expression in response to small changes in morphogen signal. Thus the signal needs amplification, but this potentially increases noise. Such spatial

stochastic dynamics of morphogens are poorly studied in any system. How does a single morphogen specify multiple gene expression boundaries?

This problem is acute in the embryonic hindbrain, where up to seven rhombomere boundaries need to sharpen. Initially each boundary is very rough, forming a transition zone of several cell diameters (Fig. 5A). Do cells within these zones sort themselves into the appropriate domains or do they show “plasticity,” switching their gene expression to match their neighbors? This has been particularly well investigated for the boundaries between r3/4 and r4/5, which in zebrafish form at 10–10.7 hpf and progressively sharpen by 12.0 hpf, as evidenced by the expression of *krox20* in r3 and r5. Clearly some sorting occurs, as demonstrated recently by tracking of *krox20*⁺ cells (Calzolari, Terriente, & Pujades, 2014; Terriente & Pujades, 2015), and previous studies have demonstrated critical roles for Ephrin/Eph signaling in repulsive interactions between cells that drive sorting (Cooke et al., 2001, Cooke, Kemp, & Moens, 2005). However, are they sufficient to sharpen the transition zones found in the developing hindbrain?

Interestingly both *Hoxb1* and *Krox20* activate their own transcription as well as mutually repressing one another (Bouchoucha et al., 2013), thereby forming a gene regulatory cassette, which creates three possible stable states within a cell, either one or the other gene is activated or both genes are off (Fig. 5B). This cassette is well suited for switching. If cellular plasticity utilizing this cassette is important for sharpening of the r4/5 boundary, gene expression studies should catch some cells coexpressing both *krox20* and *hoxb1a*, in the process of switching from the gene normally expressed on one side of the boundary to the other. This is the case; two-color double fluorescent in situ hybridization detects individual coexpressing cells (Fig. 5C) (Zhang et al., 2012). Most of these cells lie posterior to the future boundary, revealing the transition zone in which switching occurs.

Both *hoxb1a* and *krox20* are induced by RA (*hoxb1a* is a direct transcriptional target), as well as by other signals in the vicinity. In zebrafish, RA first induces *hoxb1a* up to the r3/4 boundary, with subsequent *krox20* expression initiated in r3, followed by expression in r5. A computational model incorporating (1) this temporal sequence of expression, (2) the *hoxb1/krox20* feedback cassette, and (3) an anteriorly declining gradient of RA, rapidly leads to distinct domains of *hoxb1a* and *krox20* expression that resemble rhombomeres (Fig. 5D). For this model to work, autoregulation of *krox20* must be stronger than *hoxb1a*, but otherwise it is remarkable how such a simple model is sufficient to generate the pattern seen in embryos.

7. NOISE—BOTH GOOD AND BAD

Noise in RA signaling and in its target genes is expected to compromise the ability of cells to interpret their positions within the morphogen gradient or to form sharp boundaries of gene expression. To test this idea computationally, we have varied noise in each component of the system individually and run model simulations to determine its effect on sharpness of the resulting r3/4 and r4/5 boundaries (Fig. 5D). Increasing noise in RA alone leads to rough boundaries that never sharpen—an initial transition/boundary zone of seven cell diameters remains broad, no less than six cell diameters. This is not surprising.

Strikingly, however, simultaneous inclusion of noise in RA and in its target genes (eg, *krox20* and *hoxb1a*) improves sharpening—an initial transition zone of seven or eight cell diameters between rhombomeres, sharpens to one cell diameter wide (Fig. 5D). How could this occur? Based on our combined experimental and computational work in zebrafish, we propose a mechanism of “noise-induced switching” for boundary sharpening (Fig. 5B) (Schilling et al., 2012; Zhang et al., 2012). In this model, stochastic fluctuations in *hoxb1a* and *krox20* expression enable cells to transition between two steady states, from *hoxb1a*⁺ to *krox20*⁺ or vice versa, by overcoming an energetic “barrier” between states. This model is counterintuitive because it argues for a positive role for noise, and suggests that the process of boundary sharpening needs noise in gene expression to work. A similar positive role for noise has been described for cells undergoing differentiation in isolation (Kuchina, Espinar, Garcia-Ojalvo, & Suel, 2011), but it has not been appreciated for gene expression boundaries and may be a general principle.

8. OTHER BOUNDARIES AND OTHER MORPHOGENS

Many of the principles revealed from zebrafish studies of RA signaling in the hindbrain have been limited to r4 and r5, due to a focus on *krox20* and the availability of transgenics for studying these segments. Less is known about other rhombomeres, particularly r1–3 where the RA gradient is predicted to be extremely shallow. In addition, the published model’s effectiveness is limited to r4 and r5 (Zhang et al., 2012), suggesting that additional signals interact with RA to specify r1–3. These more anterior segments experience much smaller A–P differences in RA as the gradient declines. Fate mapping studies have shown that initially *hoxa1/b1*⁺ cells extend into r3 (Labalette et al., 2015). Fgf3 and Fgf8 expressed in r4 help induce *krox20* expression in neighboring rhombomeres, first in r3 and slightly later in r5, but through distinct enhancers for each segment. A Krox20 positive feedback loop subsequently maintains its own expression (Kuchina et al., 2011). Fgf3/8 also induce Sprouty4 (Spry4), which in turn inhibits downstream activation of the Fgf pathway (Labalette et al., 2011). Computational models suggest that this provides negative feedback that controls the width of r4. Similarly *Cdx* genes further posteriorly regulate the hindbrain (r7)-spinal cord boundary through interactions with RA signaling (Chang, Skromne, & Ho, 2016; Lee & Skromne, 2014; Skromne, Thorsen, Hale, Prince, & Ho, 2007).

The most thoroughly studied morphogen in zebrafish is Nodal signaling, and recent evidence hints at a dynamic system with similar principles to that of RA in terms of gradient shape, robustness, and timing of target gene expression. Graded Nodal signaling induces the formation of germ layers as well as the dorsal–ventral (D–V) axis of the embryo (Muller et al., 2012; Sampath & Robertson, 2016; Schier, 2009; Xu, Houssin, Ferri-Lagneau, Thisse, & Thisse, 2014). Of two nodal-related genes in zebrafish, Squint (Sqt) functions directly at a distance (Chen & Schier, 2001). Furthermore Sqt induces its inhibitor, Lefty1, which forms a gradient over a greater distance than the activator Nodal, as shown using GFP- or Dendra-tagged proteins, thereby forming a classic reaction-diffusion system (Meinhardt, 2009, 2015; Muller et al., 2012). Attempts to visualize the Nodal gradient have also used reporters such as Smad2:Venus as well as bimolecular fluorescence complementation to visualize the complex between Smad2 and Smad4 (Harvey & Smith, 2009). The response to a Nodal morphogen gradient in the early zebrafish embryo appears to be dictated by the timing of

target gene induction, as determined by the activation of Smad2 and the expression kinetics of short- and long-range target genes (Dubrulle et al., 2015). In addition, studies using a zebrafish Nodal biosensor as well as immunofluorescence for phosphorylated Smad2 suggest that Nodal does not diffuse long distances, and that a temporal window for signal activation controls Nodal signaling domains (van Boxtel et al., 2015). Thus like RA, the Nodal morphogen gradient is shaped by feedback (self-enhanced inhibition) and rather than depending simply on morphogen levels, it depends on the kinetics of target gene induction.

CONCLUSIONS AND PERSPECTIVES

In this review, we have focused on the regulation of RA signaling and new methods for visualizing RA morphogen gradients in zebrafish. These studies highlight the fact that Wolpert's morphogen model only touches the tip of the iceberg in terms of morphogen dynamics and precision. Guided by computational models that reveal constraints in the system, experimental work with RA reporters in zebrafish has revealed that two factors, Cyp26a1 and Crabp2a, stand out as critical for the RA gradient. Self-enhanced degradation through Cyp26a1, as well as Crabp2a, help fine-tune RA levels within responding cells and binding of RA receptors. These allow the RA gradient to be surprisingly precise, robust, and able to induce sharp boundaries of target gene expression. However, these mechanisms cannot account for all of the robustness in the system, eg, self-enhanced degradation can compensate for twofold changes in RA synthesis, but zebrafish embryos are robust to at least 10-fold changes in RA concentration. Future studies are needed to identify the other mechanisms that account for this remarkable adaptability. The availability of GEPRAs reporters for RA availability now make it possible to correlate these features with the spatial distribution of RA in embryos.

Computational models also reveal a surprising beneficial role for noise in boundary sharpening–noise-induced switching. While RA reporters (including GEPRAs) have kinetics that are too slow to visualize noise in RA signaling directly, new methods (eg, FLIM imaging of RA autofluorescence) on the horizon should overcome this limitation. Similarly evidence to date for noise in gene expression (eg, *hoxb1a* and *krox20*) has relied on nonquantitative methods such as in situ hybridization. Recently developed quantitative in situ methods (Choi et al., 2010) as well as live imaging methods to examine the dynamic regulation of gene expression by visualizing nascent transcripts via MS2 RNA stem loops promise to reveal the details of such dynamic expression (Bothma et al., 2014). Future studies will determine if similar noise-induced switching mechanisms control sharpening boundaries of target gene expression in response to other morphogens.

Acknowledgments

We thank Pierre Le Pabic for critical comments on the manuscript. TS and QN were supported by the National Institutes of Health grants R01-GM107264, R01DE023050 and P50-GM76516. QN was also supported by National Science Foundation grant DMS1161621.

References

- Alexander C, Zuniga E, Blitz IL, Wada N, Le Pabic P, Javidan Y, ... Schilling TF. Combinatorial roles for BMPs and endothelin 1 in patterning the dorsal-ventral axis of the craniofacial skeleton. *Development*. 2011; 138:5135–5146. <http://dx.doi.org/10.1242/dev.067801>. [PubMed: 22031543]
- Alexandre C, Baena-Lopez A, Vincent JP. Patterning and growth control by membrane-tethered Wingless. *Nature*. 2014; 505:180–185. [PubMed: 24390349]
- Astrom A, Tavakkol A, Pettersson U, Cromie M, Elder JT, Voorhees JJ. Molecular cloning of two human cellular retinoic acid-binding proteins (CRABP). Retinoic acid-induced expression of CRABP-II but not CRABP-I in adult human skin in vivo and in skin fibroblasts in vitro. *Journal of Biological Chemistry*. 1991; 266:17662–17666. [PubMed: 1654334]
- Balasubramanian, R.; Zhang, X. Mechanisms of FGF gradient formation during embryogenesis. *Seminars in Cell and Developmental Biology*. 2015. <http://dx.doi.org/10.1016/j.semcdb.2015.10.004>. pii:S1084–9521(15)00189-5
- Begemann G, Schilling TF, Rauch GJ, Geisler R, Ingham PW. The zebrafish neckless mutation reveals a requirement for raldh2 in mesodermal signals that pattern the hindbrain. *Development*. 2001; 128:3081–3094. [PubMed: 11688558]
- Ben-Zvi D, Barkai N. Scaling of morphogen gradients by an expansion-repression integral feedback control. *Proceedings of the National Academy of Sciences of the United States of America*. 2010; 107:6924–6929. <http://dx.doi.org/10.1073/pnas.0912734107>. [PubMed: 20356830]
- Ben-Zvi D, Shilo BZ, Barkai N. Scaling of morphogen gradients. *Current Opinion in Genetics and Development*. 2011; 21:704–710. <http://dx.doi.org/10.1016/j.gde.2011.07.011>. [PubMed: 21873045]
- Bokel C, Brand M. Generation and interpretation of FGF morphogen gradients in vertebrates. *Current Opinion in Genetics and Development*. 2013; 23:415–422. <http://dx.doi.org/10.1016/j.gde.2013.03.002>. [PubMed: 23669552]
- Bothma JP, Garcia HG, Esposito E, Schlissel G, Gregor T, Levine M. Dynamic regulation of eve stripe 2 expression reveals transcriptional bursts in living *Drosophila* embryos. *Proceedings of the National Academy of Sciences of the United States of America*. 2014; 111:10598–10603. <http://dx.doi.org/10.1073/pnas.1410022111>. [PubMed: 24994903]
- Bouchoucha YX, Reingruber J, Labalette C, Wassef MA, Thierion E, Desmarquet-Trin Dinh C, ... Charnay P. Dissection of a Krox20 positive feedback loop driving cell fate choices in hindbrain patterning. *Molecular Systems Biology*. 2013; 9:690. <http://dx.doi.org/10.1038/msb.2013.46>. [PubMed: 24061538]
- van Boxtel AL, Chesebro JE, Heliot C, Ramel MC, Stone RK, Hill CS. A temporal window for signal activation dictates the dimensions of a Nodal signaling domain. *Developmental Cell*. 2015; 35:175–185. <http://dx.doi.org/10.1016/j.devcel.2015.09.014>. [PubMed: 26506307]
- Briscoe J, Small S. Morphogen rules: design principles of gradient-mediated embryo patterning. *Development*. 2015; 142:3996–4009. [PubMed: 26628090]
- Budhu A, Gillilan R, Noy N. Localization of the RAR interaction domain of cellular retinoic acid binding protein-II. *Journal of Molecular Biology*. 2001; 305:939–949. [PubMed: 11162104]
- Budhu AS, Noy N. Direct channeling of retinoic acid between cellular retinoic acid binding protein II and retinoic acid receptor sensitizes mammary carcinoma cells to retinoic acid-induced growth arrest. *Molecular and Cellular Biology*. 2002; 22:2632–2641. [PubMed: 11909957]
- Cai AQ, Radtke K, Linville A, Lander AD, Nie Q, Schilling TF. Cellular retinoic acid-binding proteins are essential for hindbrain patterning and signal robustness in zebrafish. *Development*. 2012; 139:2150–2155. [PubMed: 22619388]
- Calzolari S, Terriente J, Pujades C. Cell segregation in the vertebrate hindbrain relies on actomyosin cables located at the interhombomeric boundaries. *EMBO Journal*. 2014; 33:686–701. <http://dx.doi.org/10.1002/embj.201386003>. [PubMed: 24569501]
- Chang, J.; Skromne, I.; Ho, RK. CDX4 and retinoic acid interact to position the hindbrain-spinal cord transition. *Developmental Biology*. 2016. <http://dx.doi.org/10.1016/j.ydbio.2015.12.025>. pii:S0012–1606(15)30378-X

- Chen Y, Schier AF. The zebrafish Nodal signal Squint functions as a morphogen. *Nature*. 2001; 411:607–610. [PubMed: 11385578]
- Choi HM, Chang JY, Trinhle A, Padilla JE, Fraser SE, Pierce NA. Programmable in situ amplification for multiplexed imaging of mRNA expression. *Nature Biotechnology*. 2010; 28:1208–1212. <http://dx.doi.org/10.1038/nbt.1692>.
- Cooke J, Moens C, Roth L, Durbin L, Shiomi K, Brennan C, ... Holder N. Eph signaling functions downstream of Val to regulate cell sorting and boundary formation in the caudal hindbrain. *Development*. 2001; 128:571–580. [PubMed: 11171340]
- Cooke JE, Kemp HA, Moens CB. EphA4 is required for cell adhesion and rhombomere boundary formation in the zebrafish. *Current Biology*. 2005; 15:536–542. [PubMed: 15797022]
- Delva L, Bastie JN, Rochette-Egly C, Kraiba R, Balitrand N, Despouy G, ... Chomienne C. Physical and functional interactions between cellular retinoic acid binding protein II and the retinoic acid-dependent nuclear complex. *Molecular and Cellular Biology*. 1999; 19:7158–7167. [PubMed: 10490651]
- Driever W, Nusslein-Volhard C. A gradient of bicoid protein in *Drosophila* embryos. *Cell*. 1988a; 54:83–93. [PubMed: 3383244]
- Driever W, Nusslein-Volhard C. The bicoid protein determines position in the *Drosophila* embryo in a concentration-dependent manner. *Cell*. 1988b; 54:95–104. [http://dx.doi.org/10.1016/0092-8674\(88\)90183-3](http://dx.doi.org/10.1016/0092-8674(88)90183-3). [PubMed: 3383245]
- Dubrulle, J.; Jordan, BM.; Akhmetova, L.; Farrell, JA.; Kim, SH.; Solnica-Krezel, L.; Schier, AF. Response to Nodal morphogen gradient is determined by the kinetics of target gene induction; *eLife*. 2015. p. 4 <http://dx.doi.org/10.7554/eLife.05042>
- Eldar A, Rosin D, Shilo BZ, Barkai N. Self-enhanced ligand degradation underlies robustness of morphogen gradients. *Developmental Cell*. 2003; 5:635–646. [PubMed: 14536064]
- Elowitz MB, Levine AJ, Siggia ED, Swain PS. Stochastic gene expression in a single cell. *Science*. 2002; 297:1183–1186. [PubMed: 12183631]
- Grimm O, Coppéy M, Wieschaus E. Modeling the bicoid gradient. *Development*. 2010; 137:2253–2264. <http://dx.doi.org/10.1242/dev.032409>. [PubMed: 20570935]
- Harvey, SA.; Smith, JC. Visualisation and quantification of morphogen gradient formation in the zebrafish; *PLoS Biology*. 2009. p. e1000101 <http://dx.doi.org/10.1371/journal.pbio.1000101>
- Hernandez RE, Putzke AP, Myers JP, Margaretha L, Moens CB. Cyp26 enzymes generate the retinoic acid response pattern necessary for hindbrain development. *Development*. 2007; 134:177–187. [PubMed: 17164423]
- Horinaka K, Morishita Y. Encoding and decoding of positional information in morphogen-dependent patterning. *Current Opinion in Genetics and Development*. 2012; 22:553–561. [PubMed: 23200115]
- Huang W, Wang G, Delaspre F, del Vitery MC, Beer RL, Parsons MJ. Retinoic acid plays an evolutionarily conserved and biphasic role in pancreas development. *Developmental Biology*. 2014; 394:83–93. <http://dx.doi.org/10.1016/j.ydbio.2014.07.021>. [PubMed: 25127993]
- Kaern M, Elston TC, Blake WJ, Collins JJ. Stochasticity in gene expression: from theories to phenotypes. *Nature Reviews Genetics*. 2005; 6:451–464.
- Kepler TB, Elston TC. Stochasticity in transcriptional regulation: origins, consequences and mathematical representations. *Biophysical Journal*. 2001; 81:3116–3136. [PubMed: 11720979]
- Kuchina A, Espinar L, Garcia-Ojalvo J, Suel GM. Reversible and noisy progression towards a commitment point enables adaptable and reliable cellular decision making. *PLoS Computational Biology*. 2011; 7:e1002273. [PubMed: 22102806]
- Kudoh T, Wilson SW, Dawid EB. Distinct roles for Fgf, Wnt and retinoic acid in posteriorizing the neural ectoderm. *Development*. 2002; 129:4335–4346. [PubMed: 12183385]
- Labalette C, Bouchoucha YX, Wassef MA, Gongal PA, Le Men J, Becker T, ... Charnay P. Hindbrain patterning requires fine-tuning of early krox20 transcription by Sprouty 4. *Development*. 2011; 138:317–326. [PubMed: 21177344]
- Labalette C, Wassef MA, Desmarquet-Trin Dinh C, Bouchoucha YX, Le Men J, Charnay P, Gilardi-Hebenstreit P. Molecular dissection of segment formation in the developing hindbrain. *Development*. 2015; 142:185–195. [PubMed: 25516974]

- Lampron C, Rochette-Egly C, Gorry P, Dolle P, Mark M, Lufkin T, ... Chambon P. Mice deficient in cellular retinoic acid binding protein II (CRABPII) or in both CRABPI and CRABPII are essentially normal. *Development*. 1995; 121:539–548. [PubMed: 7768191]
- Lander AD. Morpheus unbound: reimagining the morphogen gradient. *Cell*. 2007; 128:245–256. [PubMed: 17254964]
- Lee K, Skromne I. Retinoic acid regulates size, pattern and alignment of tissues at the head-trunk transition. *Development*. 2014; 141:4375–4384. <http://dx.doi.org/10.1242/dev.109603>. [PubMed: 25371368]
- Li J, Hu P, Li K, Zhao Q. Identification and characterization of a novel retinoic acid response element in zebrafish *cyp26a1* promoter. *Anatomical Record*. 2012; 295:268–277. <http://dx.doi.org/10.1002/ar.21520>.
- Lumsden A, Keynes R. Segmental patterns of neuronal development in the chick hindbrain. *Nature*. 1989; 337:424–428. [PubMed: 2644541]
- Mandal A, Rydeen A, Anderson J, Sorrell MR, Zygmunt T, Torres-Vazquez J, Waxman JS. Transgenic retinoic acid sensor lines in zebrafish indicate regions of available retinoic acid. *Developmental Dynamics*. 2013; 242:989–1000. <http://dx.doi.org/10.1002/dvdy.23987>. [PubMed: 23703807]
- Meinhardt H. Models for the generation and interpretation of gradients. *Cold Spring Harbor Perspectives in Biology*. 2009; 1:a001362. [PubMed: 20066097]
- Meinhardt H. Models for patterning primary embryonic body axes: the role of space and time. *Seminars in Cell and Developmental Biology*. 2015; 42:103. <http://dx.doi.org/10.1016/j.semcdb.2015.06.005>. [PubMed: 26126935]
- Muller, P.; Rogers, KW.; Jordan, BM.; Lee, JS.; Robson, D.; Ramanathan, S.; Schier, AF. Differential diffusivity of Nodal and Lefty underlies a reaction-diffusion patterning system. *Science*. 2012. <http://dx.doi.org/10.1126/science.1221920>
- Niederreither K, Vermot J, Schuhbauer B, Chambon P, Dolle P. Retinoic acid synthesis and hindbrain patterning in the mouse embryo. *Development*. 2000; 127:75–85. [PubMed: 10654602]
- Perz-Edwards A, Hardison NL, Linney E. Retinoic acid-mediated gene expression in transgenic reporter zebrafish. *Developmental Biology*. 2001; 229:89–101. [PubMed: 11133156]
- Prols, F.; Sagar, Scaal, M. Signaling filopodia in vertebrate embryonic development. *Cellular and Molecular Life Sciences*. 2015. <http://dx.doi.org/10.1007/00018-015-2097-6>
- Ramel MC, Hill CS. The ventral to dorsal BMP activity gradient in the early zebrafish embryo is determined by graded expression of BMP ligands. *Developmental Biology*. 2013; 378:170–182. <http://dx.doi.org/10.1016/j.ydbio.2013.03.003>. [PubMed: 23499658]
- Rhinn M, Dolle P. Retinoic acid signaling during development. *Development*. 2012; 139:843–858. [PubMed: 22318625]
- Rossant J, Zirngibl R, Cado D, Shago M, Giguere V. Expression of a retinoic acid response element-hsplacZ transgene defines specific domains of transcriptional activity during mouse embryogenesis. *Genes and Development*. 1991; 5:1333–1344. [PubMed: 1907940]
- Sampath, K.; Robertson, EJ. Keeping a lid on nodal: transcriptional and translational repression of nodal signaling. *Open Biology*. 2016. <http://dx.doi.org/10.1098/rsob.150200>. pii: 150200
- Sample C, Shvartsman SY. Multiscale modeling of diffusion in the early *Drosophila* embryo. *Proceedings of the National Academy of Sciences of the United States of America*. 2010; 107:10092–10096. <http://dx.doi.org/10.1073/pnas.1001139107>. [PubMed: 20479267]
- Schier AF. Nodal morphogens. *Cold Spring Harbor Perspectives in Biology*. 2009; 1:a003459. <http://dx.doi.org/10.1101/chsperspect.a003459>. [PubMed: 20066122]
- Schilling TF, Nie Q, Lander AD. Dynamics and precision in retinoic acid morphogen gradients. *Current Opinion in Genetics and Development*. 2012; 22:562–569. <http://dx.doi.org/10.1016/j.gde.2012.11.012>. [PubMed: 23266215]
- Shimozono S, Imura T, Kitaguchi T, Higashijima S, Miyawaki A. Visualization of an endogenous retinoic acid gradient across embryonic development. *Nature*. 2013; 496:363–366. <http://dx.doi.org/10.1038/nature12037>. [PubMed: 23563268]
- Sirbu IO, Gresh L, Barra J, Duester G. Shifting boundaries of retinoic acid activity control hindbrain segmental gene expression. *Development*. 2005; 132:2611–2622. [PubMed: 15872003]

- Skromne I, Thorsen D, Hale M, Prince VE, Ho RK. Repression of the hindbrain developmental program by Cdx factors is required for the specification of the vertebrate spinal cord. *Development*. 2007; 134:2147–2158. [PubMed: 17507415]
- Stathopoulos A, Iber D. Studies of morphogens: keep calm and carry on. *Development*. 2013; 140:4119–4124. [PubMed: 24086076]
- Strigini M, Cohen SM. Wingless gradient formation in the *Drosophila* wing. *Current Biology*. 2000; 10:293–300. [PubMed: 10744972]
- Stringari C, Cinquin A, Cinquin O, Digman MA, Donovan PJ, Gratton E. Phasor approach to fluorescence lifetime microscopy distinguishes different metabolic states of germ cells in a live tissue. *Proceedings of the National Academy of Sciences of the United States of America*. 2011; 108:13582–13587. <http://dx.doi.org/10.1073/pnas.1108161108>. [PubMed: 21808026]
- Terriente J, Pujades C. Cell segregation in the vertebrate hindbrain: a matter of boundaries. *Cellular and Molecular Life Sciences*. 2015; 72:3721–3730. [PubMed: 26089248]
- Tickle C, Summerbell D, Wolpert L. Positional signaling and specification of digits in chick limb morphogenesis. *Nature*. 1975; 254:199–202. [PubMed: 1113884]
- Trevarrow B, Marks DL, Kimmel CB. Organization of hindbrain segments in the zebrafish embryo. *Neuron*. 1990; 4:669–679. [PubMed: 2344406]
- Tuazon FB, Mullins MC. Temporally coordinated signals progressively pattern the anteroposterior and dorsoventral body axes. *Seminars in Cell and Developmental Biology*. 2015; 42:118–133. [PubMed: 26123688]
- Umulis DM, Shimmi O, O'Connor MB, Othmer HG. Organism-scale modeling of early *Drosophila* patterning via bone morphogenetic proteins. *Developmental Cell*. 2010; 18:260–274. <http://dx.doi.org/10.1016/devcel.2010.01.006>. [PubMed: 20159596]
- Wartlick O, Kicheva A, Gonzalez-Galtan M. Morphogen gradient formation. *Cold Spring Harbor Perspectives in Biology*. 2009; 1:a001255. [PubMed: 20066104]
- Waxman JS, Yelon D. Zebrafish retinoic acid receptors as context dependent transcriptional activators. *Developmental Biology*. 2011; 352:128–140. [PubMed: 21276787]
- White RJ, Nie Q, Lander AD, Schilling TF. Complex regulation of *cyp26a1* creates a robust retinoic acid gradient in the zebrafish embryo. *PLoS Biology*. 2007; 5:e304. [PubMed: 18031199]
- White RJ, Schilling TF. How degrading: Cyp26s in hindbrain development. *Developmental Dynamics*. 2008; 237:2775–2790. <http://dx.doi.org/10.1002/dvdy.21695>. [PubMed: 18816852]
- Xiong F, Tentner AR, Huang P, Gelas A, Mosaliganti KR, Souhait L, ... Megason SG. Specified neural progenitors sort to form sharp domains after noisy Shh signaling. *Cell*. 2013; 153:550–561. [PubMed: 23622240]
- Xu PF, Houssin N, Ferri-Lagneau KF, Thisse B, Thisse C. Construction of a vertebrate embryo from two opposing morphogen gradients. *Science*. 2014; 344:87–89. <http://dx.doi.org/10.1126/science.1248252>. [PubMed: 24700857]
- Zhang L, Radtke K, Zheng L, Cai AQ, Schilling TF, Nie Q. Noise drives sharpening of gene expression boundaries in the zebrafish hindbrain. *Molecular Systems Biology*. 2012; 8:613. [PubMed: 23010996]

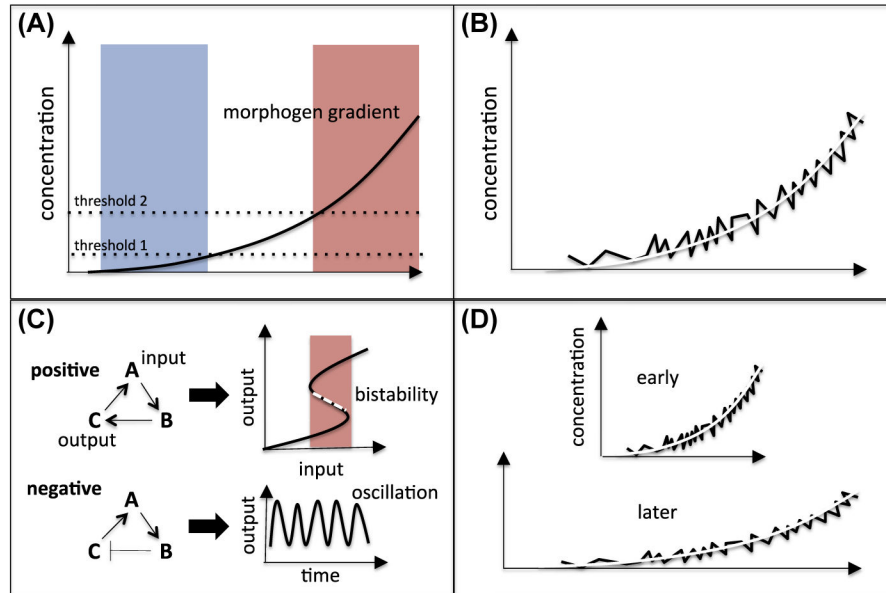


FIGURE 1. Morphogen dynamics and regulation

(A) Standard representation of a morphogen gradient, adapted from L Wolpert’s “French flag” model. The *solid line* denotes the morphogen concentration (Y axis)—highest at its source to the right of a field of responding cells (X axis). *Dotted lines* denote concentration thresholds at which cells respond differently. Blue, white, and red regions represent three distinct cell fates. (B) Hypothetical noisy morphogen gradient (*black line*) that on average matches its smooth counterpart (*white line*). (C) Examples of positive and negative feedback on signal output. Through positive feedback, a given variable input (A—X axis in graph) can result in two stable outputs (Y axis in graph), with an intervening transition state (red). Similar input driving negative feedback can result in signal oscillations over time (X axis). (D) Scaling of a morphogen gradient as the field of cells over which it acts grows (X-axis). (See color plate)

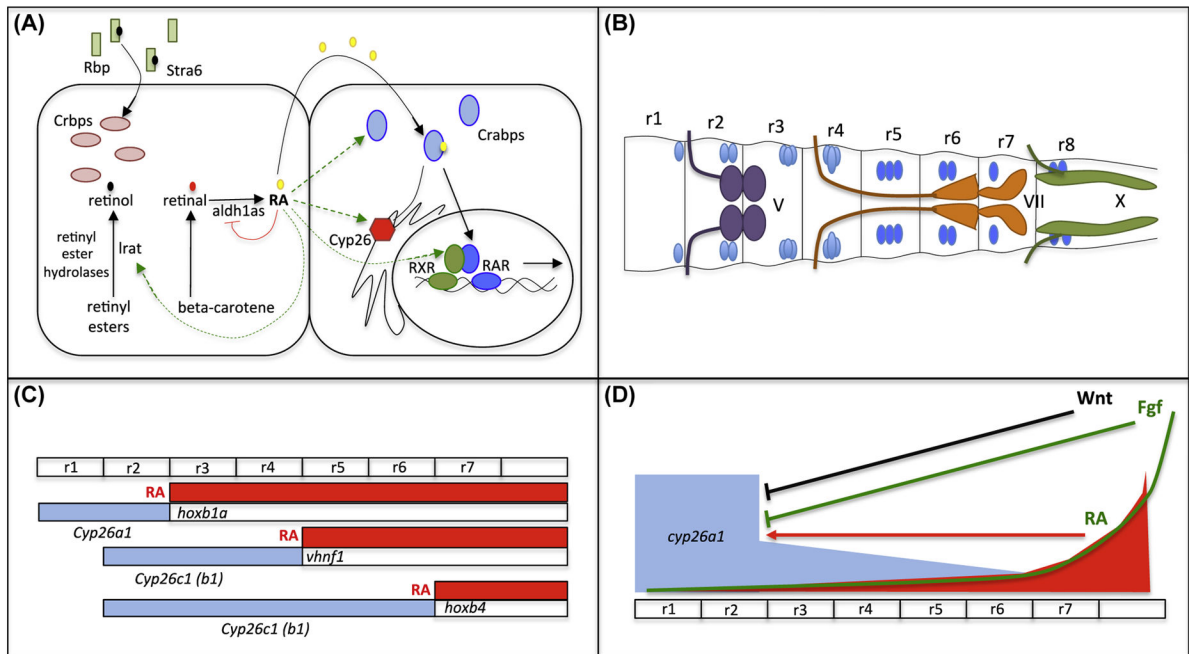


FIGURE 2. Retinoic acid (RA) as a morphogen in hindbrain patterning

(A) Feedback in RA signaling. Signaling cell (left), responding cell (right). Vitamin A (retinol) transported by retinol-binding proteins (Rbps, *light green rectangles*) and Stra6 into cells or derived from retinyl esters via Lrat, associates with cellular retinol-binding proteins (Crbps, *light red ovals*). Retinol (black) is converted to retinal (red) and then to RA (yellow) by aldehyde dehydrogenases (Aldh1as). RA travels within cells bound to cellular RA-binding proteins (Crabps, *light blue ovals*), either to the nucleus to bind RARs (*blue ovals*) or to Cyp26s (red hexagon) associated with endoplasmic reticulum for degradation. Known positive (green, *dashed arrows*) feedback within the pathway includes Lrat, Crabps, Cyp26s, and RARs. Known negative (*red lines*) feedback includes Aldh1a2. (B) Rhombomeric organization in zebrafish. Eight rhombomeres (r1–8, anterior to the left) contain distinct sets of interneurons (blue) and motor neurons (V, trigeminal, purple; VII, facial, orange; X, vagal, green). (C) Shifting boundaries of RA degradation and hindbrain patterning based on RARE:lacZ transgenic reporters in mice. Model depicting rhombomeres at top, Cyp26s in blue, RA in red. An early Cyp26a1 domain sets the r2/3/*hoxb1a* expression boundary, a later Cyp26c1 (b1 in zebrafish) sets the r4/5/*vhnf1* expression boundary, and Cyp26c1 expands posteriorly to demarcate the r6/7/*hoxb4* boundary. (D) An integrated signaling network for hindbrain patterning. Model depicting rhombomeres at bottom, Cyp26a1 in blue, RA signaling in red, Fgf signaling in green, Wnt signaling in black. Cyp26-mediated degradation is continuously under feedback and feedforward control from Wnt, Fgf, and RA signaling, respectively, which shapes the RA gradient. (See color plate)

Adapted from White, R.J. & Schilling, T.F. (2008). How degrading: Cyp26s in hindbrain development. *Developmental Dynamics*, 237, 2775–2790. <http://dx.doi.org/10.1002/dvdy.21695> and Schilling, T.F., Nie, Q. & Lander, A.D. (2012). Dynamics and precision in retinoic acid morphogen gradients. *Current Opinion in Genetics and Development*, 22, 562–569. <http://dx.doi.org/10.1016/j.gde.2012.11.012>.

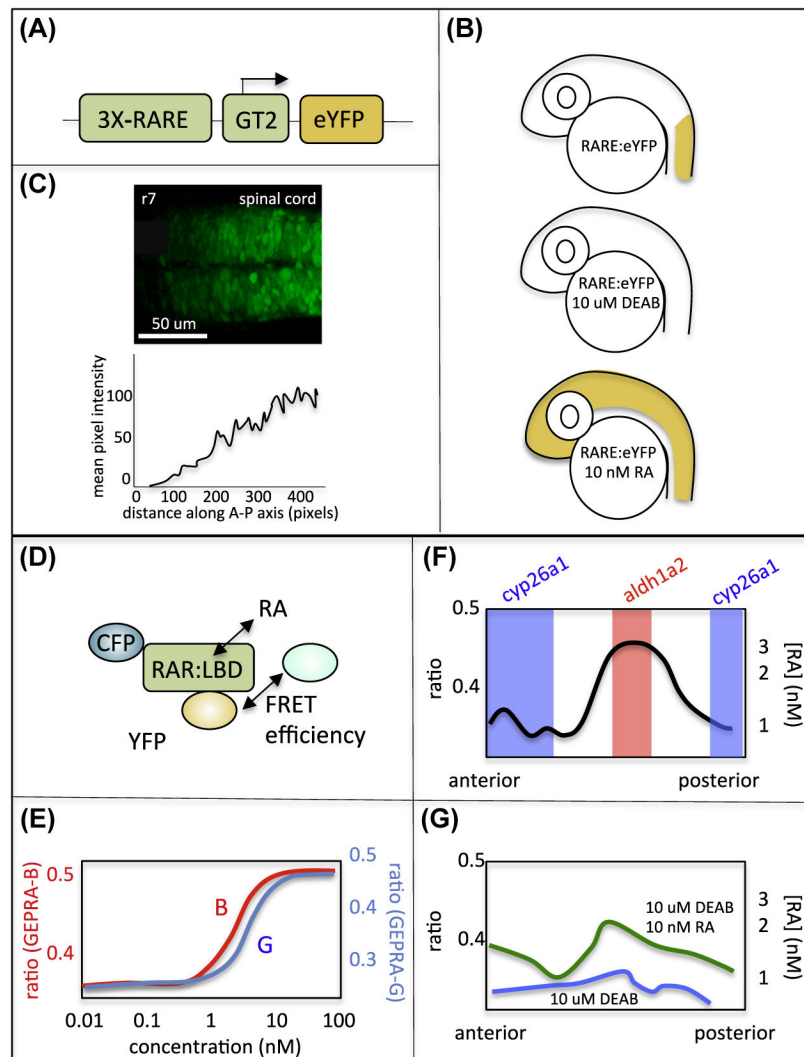


FIGURE 3. Visualizing the Retinoic acid (RA) morphogen gradient

(A) Construct (RARE:eYFP) most commonly used to monitor RA signaling in zebrafish, containing three RA response elements (RAREs) from the mouse RAR β gene, a GATA-2 basal promoter (GT2), and an enhanced yellow fluorescent protein (eYFP) (Perz-Edwards et al., 2001). (B) RARE:eYFP transgenic zebrafish embryos show expression in the spinal cord, which is lost with 10 μ M DEAB treatments and induced throughout the CNS with application of 10 nM exogenous RA. (C) Confocal image of RARE-YFP fluorescence at 24 hpf (upper panel, dorsal view, anterior to the left) and quantification of YFP fluorescence at the hindbrain/spinal cord boundary (lower panel). (Adapted from White, R.J., Nie, Q., Lander, A.D. & Schilling, T.F. (2007). *Complex regulation of cyp26a1 creates a robust retinoic acid gradient in the zebrafish embryo. PLoS Biol*, 5, e304.) (D) GEPRAs reporters based on the RAR ligand-binding domain (LBD) and fused to CFP and YFP. (E) Dose-response shows sensitivity between 1 and 10 nM of GEPRAs-B (red) and GEPRAs-G (blue) reporters. (F) Graph based on ratiometric imaging of GEPRAs fluorescence intensity measured at 12 hpf reveals graded RA levels between 0.5 and 3 nM, distributed along the anterior–posterior axis (X axis) between its source in the domain of *aldh1a2* expression (red)

and both anterior and posterior domains of *cyp26a1* expression (blue). (G) GEPRA measurements of RA levels in embryos treated with DEAB (RA depleted, *blue line*) and simultaneously treated with 10 μ M DEAB and 10 nM RA (*green line*), which partially restores the gradient. (See color plate)

Adapted from Shimozono, S., Iimura, T., Kitaguchi, T., Higashijima, S. & Miyawaki, A. (2013). Visualization of an endogenous retinoic acid gradient across embryonic development. Nature, 496, 363–366. <http://dx.doi.org/10.1038/nature12037>.

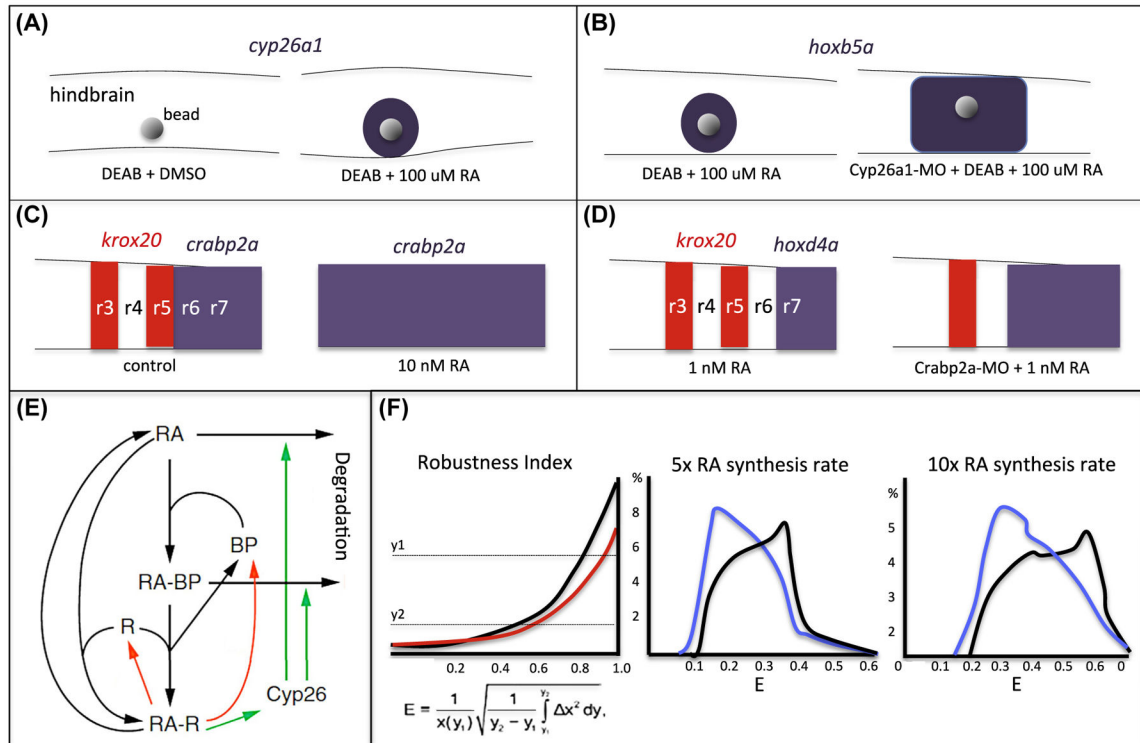


FIGURE 4. Negative feedback through Cyp26a1 and Crabp2a improve gradient robustness (A) Induction of *cyp26a1* expression (purple) by a bead soaked in 100 μM retinoic acid (RA) (right panel) implanted into the hindbrain region of a DEAB-treated embryo, in contrast to a control DMSO-soaked bead (left panel). Dorsal views, anterior to the left. (B) Induction of *hoXB5a* expression (purple) by an RA-soaked bead implanted into DEAB-treated embryos extends over a longer range in an embryo depleted of Cyp26a1 (injected with a Cyp26a1-MO). (C) Induction of *crabp2a* expression (purple) by treatment of an embryo with 10 nM RA extends throughout the hindbrain and correlates with loss of markers of anterior rhombomeres such as *kroX20* (red) in r3 and r5. (D) Induction of *hoXd4a* expression (purple) by treatment with 1 nM RA extends up to the r4/5 boundary in an embryo depleted of Crabp2a (injected with a Crabp2a-MO). (E) Bound and unbound states of RA within responding cells and paths to degradation, which are included in computational models. (F) Left graph, robustness index (E—formula shown below) comparing experimental (red) and reference (black) gradients by where they cross two thresholds (y_1 , y_2). Right graphs show two examples of probability density distributions (percentages, Y axis) of E values (X axis) for models that either include binding proteins (blue lines) or do not (black lines) with either a 5-fold or 10-fold increase in RA synthesis rate. (See color plate)

Adapted from White, R.J., Nie, Q., Lander, A.D. & Schilling, T.F. (2007). Complex regulation of *cyp26a1* creates a robust retinoic acid gradient in the zebrafish embryo. PLoS Biology, 5, e304 and Cai, A.Q., Radtke, K., Linville, A., Lander, A.D., Nie, Q. & Schilling, T.F. (2012). Cellular retinoic acid-binding proteins are essential for hindbrain patterning and signal robustness in zebrafish. Development, 139, 2150–2155.

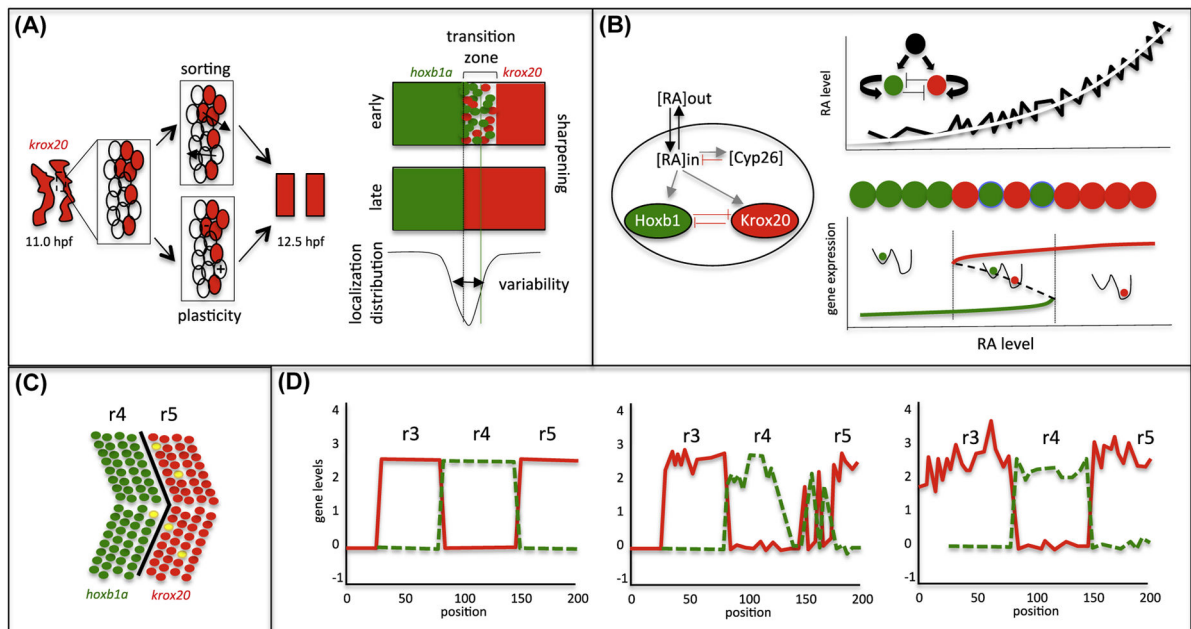


FIGURE 5. Noise-induced switching and boundary sharpening in response to retinoic acid (RA)

(A) Rhombomere boundary sharpening. Hypothetical roles of cell sorting versus plasticity in sharpening of two stripes of *krox20* expression (red) in r3 and r5 in a zebrafish embryonic hindbrain (dorsal view) between 11.0 and 12.5 hpf (left panel). Model depicting sharpening of the “transition zone” between two rhombomeres (r4, *hoxb1a*, green; r5, *krox20*, red), which normally occurs posterior to the final boundary (dashed black line) and contains cells expressing both genes. Green line indicates alternate boundary that can form if sharpening occurs at a more posterior position. (B) Noise-induced switching at the r4/5 boundary. (left panel) The model includes extracellular RA levels (RA)_{out}, intracellular levels (RA)_{in}, self-enhanced degradation through Cyp26a1 induction, and mutual inhibition between Hoxb1 and Krox20. (upper right panel) RA fluctuations combined with the gene regulatory network lead to fluctuations in target gene expression (green and red cells) near the boundary. (lower right panel) Noise in gene expression helps push cells into one of two stable states in the bistable region (green to red). (C) Evidence for an r4/5 transition zone. Diagram of double fluorescent in situ hybridization experiments demonstrating cells coexpressing *hoxb1a* (green) and *krox20* (red), largely posterior to the future boundary. (D) Modeling suggests that noise-induced switching improves sharpening. Simulations using the model shown in B resolve into rhombomere-like domains of gene expression (Y axis) along a 200- μ m stretch along the anterior–posterior axis (X axis) (left graph). Noise in (RA)_{in} alone results in failure of r4/5 boundary to sharpen (middle graph). Noise in both (RA)_{in} and in gene expression restores sharpening (right graph). (See color plate)

Adapted from Zhang, L., Radtke, K., Zheng, L., Cai, A.Q., Schilling, T.F. & Nie, Q. (2012). *Noise drives sharpening of gene expression boundaries in the zebrafish hindbrain*. *Molecular Systems Biology*, 8, 613 and Schilling, T.F., Nie, Q. & Lander, A.D. (2012). *Dynamics and precision in retinoic acid morphogen gradients*. *Current Opinion in Genetics and Development*, 22, 562–569. <http://dx.doi.org/10.1016/j.gde.2012.11.012>.

Table 1

Transgenic RA Reporters in Zebrafish

Reporter	Promoter	Advantages	Disadvantages	References
3xRARE:YFP	GATA-2 (GT2)	sensitive (nM)	dim; late onset (13 hpf)	Perz-Edwards et al. (2001)
3xRARE:GFP	thymidine kinase (tk)	sensitive (nM)	dim; late onset (13 hpf); neural tube/retina only	Perz-Edwards et al. (2001)
12xRARE: eGFP	elongation factor (ef1a)	sensitive (nM)	dim; late onset (13 hpf)	Waxman and Yelon (2011)
cyp26a1:eYFP	b-actin	sensitive (nM); early onset (8 hpf)	dim; some non-RA-dependent expression	Li et al. (2012)
GDBD-RLBD; UAS:GFP	b-actin	sensitive (nM)	dim; late onset (13 hpf)	Mandal et al. (2013)
VPBD-GDBD; UAS:GFP	b-actin	hypersensitive	hypersensitive	Mandal et al. (2013)
4xRARE-cFos: QF; QUAS: GFP	c-fos	sensitive (nM)	dim; late onset (13 hpf)	Huang et al. (2014)
GEPRAs-B/GEPRAs-G	N/A	measure (RA) quantitatively; early onset	K_a dependence; dim	Shimozono et al. (2013)

Comparison of the composition, advantages, and disadvantages of different published RA reporters. Many use concatenated RA response elements (RAREs)—5'-gggtca(n5)agttca-3'—based on the RAR β receptor in mice, with different numbers of RAREs and basal promoters (column 2). Surprisingly these all seem to have similar sensitivities in the nM range and are first detected after gastrulation, at 13 hpf. For 4RARE-cFos:QF; QUAS:GFP the RAREs were cloned upstream of a cFos minimal promoter and sequence encoding the QF transcriptional activator, and in the same transgene QF-binding upstream activating sequence drives GFP. Other reporters use the RAR ligand-binding domain (RLBD). RLBD is either fused to the Gal4 DNA-binding domain (GDBD) or a VP16-GDBD (VDBD) together with Gal4-binding upstream activating sequences (UAS) driving GFP. For Genetically Encoded Probes for RA (GEPRAs) reporters the RLBD is fused to CFP and YFP to allow monitoring of RA binding using Fluorescence Resonance Energy Transfer.